JGR Earth Surface

RESEARCH ARTICLE
10.1029/2023JF007274

Multi-Year Tracing of Spatial and Temporal Dynamics of Post-Fire Aeolian Sediment Transport Using Rare Earth Elements Provide Insights Into Grassland Management

William J. Burger[1], R. Scott Van Pelt[2], David E. Grandstaff[1], Guan Wang[3], Temuulen T. Sankey[4], Junran Li[5], Joel B. Sankey[6], and Sujith Ravi[1]

[1]Department of Earth & Environmental Science, Temple University, Philadelphia, PA, USA, [2]Wind Erosion and Water Conservation Research, USDA-ARS, Big Spring, TX, USA, [3]School of Soil and Water Conservation, Beijing Forestry University, Beijing, China, [4]School of Informatics, Computing, and Cyber Systems, Northern Arizona University, Flagstaff, AZ, USA, [5]Department of Geography, The University of Hong Kong, Hong Kong, China, [6]U.S. Geological Survey, Southwest Biological Science Center, Grand Canyon Monitoring and Research Center, Flagstaff, AZ, USA

Key Points:

- First long-term analysis of post-fire aeolian sediment transport using multiple rare earth element tracers
- Aeolian transport, fires, and vegetation modify surface processes in which distinct soils develop at very fine spatial scales of individual plants
- Demonstrates long-term changes in the post-fire shift in aeolian sediment source and sink dynamics in heterogeneous dryland landscapes

Supporting Information:

Supporting Information may be found in the online version of this article.

Correspondence to:

S. Ravi,
sravi@temple.edu

Citation:

Burger, W. J., Van Pelt, R. S., Grandstaff, D. E., Wang, G., Sankey, T. T., Li, J., et al. (2023). Multi-year tracing of spatial and temporal dynamics of post-fire aeolian sediment transport using rare earth elements provide insights into grassland management. *Journal of Geophysical Research: Earth Surface*, *128*, e2023JF007274. https://doi.org/10.1029/2023JF007274

Received 25 MAY 2023
Accepted 18 OCT 2023
Corrected 11 NOV 2023

This article was corrected on 11 NOV 2023. See the end of the full text for details.

Author Contributions:

Conceptualization: R. Scott Van Pelt, David E. Grandstaff, Temuulen T. Sankey, Junran Li, Joel B. Sankey, Sujith Ravi
Data curation: William J. Burger
Formal analysis: William J. Burger, David E. Grandstaff, Guan Wang
Funding acquisition: Junran Li, Joel B. Sankey, Sujith Ravi

Abstract Aeolian sediment transport occurs as a function of, and with feedback to ecosystem changes and disturbances. Many desert grasslands are undergoing rapid changes in vegetation, including the encroachment of woody plants, which alters fire regimes and in turn can change the spatial and temporal patterns of aeolian sediment transport. We investigated aeolian sediment transport and spatial distribution of sediment in the surface soil for 7 years following a prescribed fire using a multiple rare earth element (REE) tracer-based approach in a shrub-encroached desert grassland in the northern Chihuahuan desert. Results indicate that even though the aeolian horizontal sediment mass flux increased approximately three-fold in the first windy season in the burned areas compared to control areas, there were no significant differences after three windy seasons. The soil surface of bare microsites was the major contributor of aeolian sediments in unburned areas (87%), while the shrub microsites contributed the least (<2%) during the observation period. However, after the prescribed fire, the contribution of aeolian sediments from shrub microsites increased considerably (~40%), indicating post-fire microsite-scale sediment redistribution. The findings of this study, which is the first to use multiple REE tracers for multi-year analysis of the spatial and temporal dynamics of aeolian sediment transport, illustrate how disturbance by prescribed fire can influence aeolian processes and alters dryland soil geomorphology in which distinct soils develop over time at very fine spatial scales of individual plants.

Plain Language Summary In this study, we investigated how soil and nutrients attached to soil particles are transported and redeposited by wind after a prescribed fire using a new tracer method in a desert grassland. Results from this long-term (7-years) experiment in a desert grassland in the northern Chihuahuan desert reveal the role of fire in changing the erosional and depositional areas on the soil surface, which in turn determine what vegetation type can dominate the landscape. In a grassland encroached with shrubs, prescribed fire modified soil erosion processes and resulted in a more uniform distribution of nutrients in the landscape, favoring grass recovery. The findings also highlight the role of prescribed fires as an effective grassland management tool.

1. Introduction

Aeolian processes—the erosion, transportation, and deposition of sediment by the wind—affect landscape evolution, soil fertility, climate, and air quality (Field et al., 2010; Kok et al., 2018; Ravi et al., 2011). Aeolian sediment transport can be substantial and sometimes even the dominant geomorphic process in drylands (Breshears et al., 2003; Field et al., 2009), which comprise almost 40% of the Earth's terrestrial surface (Millennium Ecosystem Assessment, 2005). In grasslands and rangelands, which account for 65% of drylands, aeolian processes are known to interact with vegetation change and disturbances at multiple spatial and temporal scales (Li et al., 2008; Okin et al., 2006; Ravi et al., 2012; Sankey, Germino, Benner, et al., 2012; Sankey, Germino, & Glenn, 2012; Sankey, Germino, Sankey, & Hoover, 2012). Grassland degradation is often attributed to the encroachment of woody plants and associated transformative changes to the geomorphology, soils, and ecology of the grasslands (Archer, 1989; Grover & Musick, 1990; Schlesinger et al., 1990; van Auken, 2000). This phenomenon, also referred to as shrub encroachment, has been documented worldwide and many studies have investigated

Investigation: William J. Burger, David E. Grandstaff, Temuulen T. Sankey, Junran Li, Joel B. Sankey, Sujith Ravi
Methodology: R. Scott Van Pelt, David E. Grandstaff, Temuulen T. Sankey, Junran Li, Joel B. Sankey, Sujith Ravi
Project Administration: Junran Li, Joel B. Sankey, Sujith Ravi
Resources: R. Scott Van Pelt, David E. Grandstaff, Temuulen T. Sankey, Junran Li, Sujith Ravi
Supervision: Junran Li, Joel B. Sankey, Sujith Ravi
Visualization: William J. Burger, Sujith Ravi
Writing – original draft: William J. Burger, Sujith Ravi
Writing – review & editing: William J. Burger, R. Scott Van Pelt, David E. Grandstaff, Guan Wang, Temuulen T. Sankey, Junran Li, Joel B. Sankey, Sujith Ravi

the geomorphological, ecological, hydrological, and socio-economic impacts of this transformative landscape change (e.g., D'Odorico et al., 2013; Huxman et al., 2005; Turnbull et al., 2012; Wilcox, 2010).

Shrub encroachment can result from complex interactions among several factors, including but not limited to, an increase in CO_2 concentration, warming, overgrazing, fire suppression, and microclimate modification by vegetation (Archer et al., 1995; Li et al., 2022; Schlesinger et al., 1990). The abrupt transitions are often sustained by positive feedbacks between the state of the system (shrub or grass) and environmental conditions or disturbances, which can alter geomorphology and soil processes from patch to landscape scales (Okin & Gillette, 2001; Ravi et al., 2009). As vegetation is a dominant control on wind erosion from soil surfaces, changes in vegetation either through changes in compositions or disturbance regimes can alter the rates and patterns of aeolian transport (Gillette & Pitchford, 2004; Li et al., 2007; Munson et al., 2011; Wolfe & Nickling, 1993). Shrub encroachment into areas historically dominated by grasses often results in an increase in bare soil areas (Okin & Gillette, 2001) and decrease in the vegetation connectivity that propagate wildfires. An increase in the length of bare connected pathway results in the acceleration of aeolian sediment transport in the landscape (Okin et al., 2009). Aeolian processes enhance and maintain the local spatial heterogeneities in nutrient and vegetation distribution through removal of nutrient-rich sediments from interspaces and the subsequent redeposition onto shrub-vegetated areas (Okin & Gillette, 2001). Via canopy-trapping of eroded sediment, shrub vegetation biogeochemically and hydrologically enhances these shrub microsites ("islands of fertility") compared to grass and bare microsites (Charley & West, 1975; Gonzales et al., 2018; Sankey, Germino, Sankey, & Hoover, 2012; Schlesinger et al., 1990). Overall, this transition from a grassland to shrubland results in an increase in bare soil, which can then be easily eroded, accelerating the land degradation process often associated with shrub encroachment (Li et al., 2022; Schlesinger et al., 1990).

Recent studies in shrub-grass ecotones have indicated that at the early stage of encroachment, reintroduction of fires may potentially alter the feedbacks that reinforce shrub encroachment, with implications for the reversibility of shrub encroachment (Ravi et al., 2009; Wang et al., 2019). In particular, wind tunnel and plot-scale field experiments in the shrub-grass ecotone in the Northern Chihuahuan Desert have shown that aeolian sediment transport that occurs subsequent to prescribed fires can redistribute soil nutrient resources from shrub microsites, decrease vegetation and microsite heterogeneity, and decrease soil microtopography (Ravi et al., 2009; Sankey et al., 2021; Wang et al., 2019). Accelerated post-fire soil erosion from vegetated microsites was attributed to the vegetation removal and changes in soil water retention in burned soil (Doerr, et al., 2000; Ravi, D'Odorico, Zobeck, et al., 2007; Ravi et al., 2006). Overall, a homogenous redistribution of soil resources following fires may result in increased grass growth, potentially reversing land degradation induced by shrub encroachment (Ravi et al., 2009; Sankey, Ravi, et al., 2012; Wang et al., 2019).

Even though some studies have demonstrated the potential of fires to accelerate aeolian sediment transport and to redistribute sediment in the soil surface (Ravi et al., 2009; Wang et al., 2019), the long-term (annual-decadal) dynamics of post-fire aeolian sediment transport and the extent of spatial homogenization of soil surfaces across the landscape is not clear. Hence, quantifying the post-disturbance sediment–nutrient redistribution pathways is critical for understanding land degradation and soil biogeochemical cycling, and for analyzing the effects of climate change, disturbances and management scenarios on drylands. Reliable tracer-based techniques to accurately determine the rate of aeolian sediment transport and redistribution of aeolian sediment in the soil or to reconstruct the aeolian sediment source-to-sink routes over long time scales are lacking (Wang et al., 2017). Recently, Dukes et al. (2018) demonstrated the applicability of using rare earth element (REE) tracers to quantify aeolian sediment transport in desert grasslands over short time scales of one season. REEs are ideal tracers for studying aeolian sediment transport and redistribution of aeolian sediment in the soil surface because they have low mobility in predominantly alkaline soils, low toxicity, low background concentration, and bond strongly with soil particles (Deasy & Quinton, 2010; Polyakov & Nearing, 2004; Zhang et al., 2001). However, the applicability of multiple REE tracers for understanding the long-term source-sink dynamics of aeolian sediments has not been assessed before. Here, using multiple REE tracers, we investigated relationships between aeolian sediment transport and the spatial distribution of aeolian sediments in the soil surface at the individual plant microsite scale in a shrub-encroached desert grassland for 7 years following a prescribed fire. Our research question is whether aeolian sediment transport following prescribed fire implemented during the early stages of shrub encroachment can favor the local-scale redistribution of soil nutrients from the islands of fertility beneath the burned shrubs to the adjacent bare interspaces, thereby providing negative feedback to the woody plant encroachment into grasslands.

2. Study Area and Methods

2.1. Study Area

The shrub-grass transition ecotone at the Sevilleta National Wildlife Refuge (SNWR) in the Northern Chihuahuan Desert (New Mexico, USA, 34.33062°N, 106.72078°W) provides a suitable site to investigate aeolian processes and the above-mentioned feedback and to evaluate the implications of management scenarios for the state of the system. The study site was established in a shrub-grass transition zone consisting of black grama grass (*Bouteloua eriopoda*), creosote shrub (*Larrea tridentata*), and bare interspaces. The primary windy season is from February to May, with the dominant wind direction from the southwest. The site receives most of its precipitation from June to October during the North American Monsoon season (Higgins et al., 1997). The soil is characterized as a sandy loam (Dukes et al., 2018). More information on soil texture is provided in Supporting Information S1 (Table S1).

2.2. Experimental Layout

Two treatment areas (100 × 100 m each; 250 m apart) were established in March 2016: burned and control. Each treatment consisted of three 30 × 10 m replicate monitoring areas, oriented perpendicular to the dominant wind direction and 25 m apart. In the middle of each replicated monitoring area, a 5 × 5 m plot was designated for soil sampling, enough to capture the heterogeneity of the landscape, including all three microsites: bare, grass, and shrub (Figures S1 and S2 in Supporting Information S1). A prescribed burn was conducted to create the burned treatment (2016) prior to the windy season. Controlled burns are routinely performed at the SNWR as part of fire management to decrease the fuel load and eliminate invasive species and shrubs. The prescribed burn was confined inside the designated burned treatment area. Fire was ignited using propane torches (to minimize fuel residues) and allowed to spread naturally in the direction of prevailing winds. To ensure continuous fire propagation and uniform fire coverage, some shrubs had to be reignited using propane torches. A previous study (Ravi et al., 2009) from this grass-shrub transition zone showed that the average fire temperatures were typically higher beneath the shrub (~260°C) compared to grass patches (~120°C), and barely impacted soil deeper than 5 cm regardless of the aboveground vegetation.

Soil samples for laboratory analysis of chemical composition were taken before (March) and after (June) the windy season in 2016, 2017, and 2018. A 4-m-high meteorological tower was installed in each treatment. The towers were solar powered and equipped with a data logger (CR1000, Campbell Scientific, Logan, UT) and sensors to measure wind speed (Anemometer 03101-L, Campbell Scientific, Logan, UT), wind direction (Wind Sentry Set 03002-L, Campbell Scientific, Logan, UT), relative humidity, air temperature (Temperature/RH Probe CS215-L, Campbell Scientific, Logan, UT), and soil moisture (12 cm Soil Water Content Reflectometer, CS655, Campbell Scientific, Logan, UT). Wind speeds were measured at four heights: 0.5, 1.0, 2.0, and 4.0 m. All variables were recorded every second and averaged over 1-min intervals. Both control and burned treatments experienced similar wind speeds during the experimental period (Figure 1).

2.3. Aeolian Sediment Transport Monitoring

Downwind of each 5 × 5 m soil sampling plot in the replicated burned and control monitoring areas, the wind-blown sediment was collected using two custom-made Modified Wilson and Cooke (MWAC) sediment collectors. Each MWAC sampler array consisted of four aluminum bottles (for sediment collection) mounted at incremental heights (0.10, 0.25, 0.50, 0.85 m) (Dukes et al., 2018; Sterk & Raats, 1996). The deposited aeolian sediment was collected twice every year, before and after the windy season for the first 3 years of the study. A final sample collection was conducted in May 2022 (7th year).

The mass of aeolian sediment collected in the MWAC samplers during each windy season was used to calculate the total horizontal mass flux (Q) for each plot. The mass of sediment collected in each sampler bottle was divided by the area of the sampler inlet and the duration of sampling time (days) to obtain the time-averaged horizontal mass flux ($q(z)$). The values of $q(z)$ were then fitted to the empirical model used by Shao et al. (1993):

$$q(z) = ce^{(az^2+bz)} \quad (1)$$

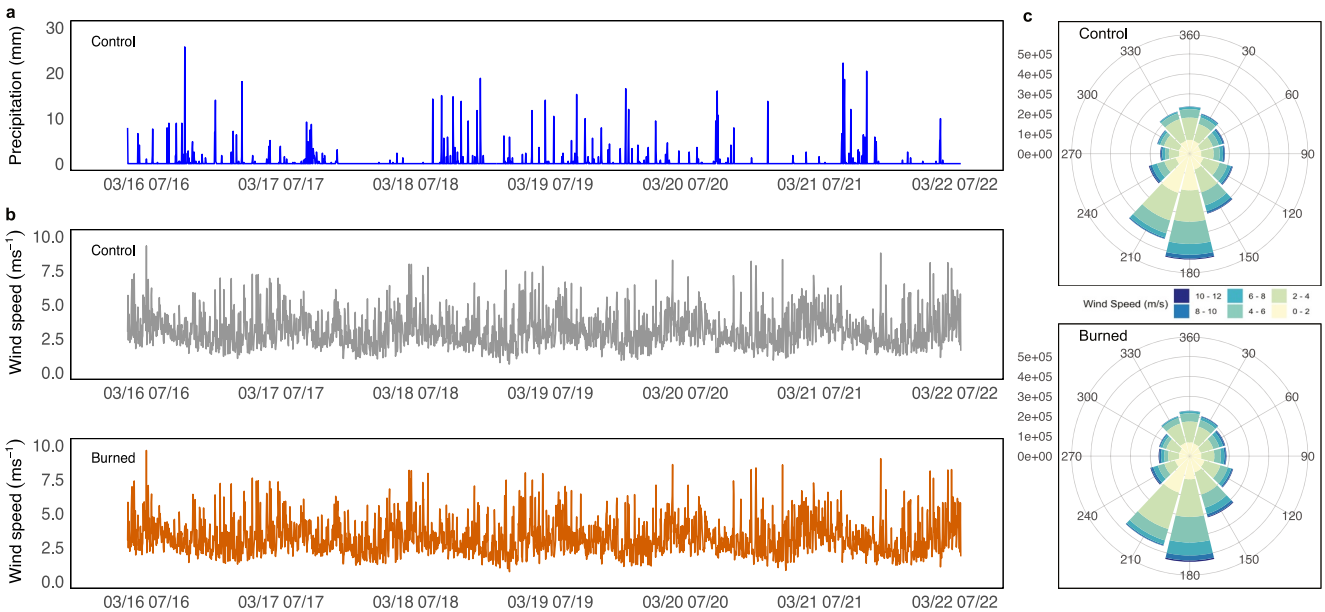

Figure 1. Time-series of (a) daily precipitation at both sites, (b) daily average wind speed values (at 4 m height) and (c) Rose diagram showing the distribution of wind directions and wind speeds (1-min average) from the control and burned areas over the 7-years experimental period. Each concentric circle represents the number of events and the length of each spoke around the circle indicates the amount of time that the wind blows from a particular direction with that speed range (colors).

where z is the height from the ground to the center of the dust sampler inlet, and a, b, and c are fitting constants. The Q over the full sampling time was calculated by integrating $q(z)$ from the ground (0 m) to a height of 1 m (Dukes et al., 2018; Li et al., 2007; Shao & Raupach, 1992):

$$Q = \int_0^{1m} q(z)\, dz \tag{2}$$

The statistical significance of the differences in Q values between control and burned flux for each sampling period was tested using Kruskal-Wallis one-way ANOVA test.

Wind velocities from the burned and control treatments over the course of the experimental period were used to derive the parameters of the wind profile, including the roughness length (z_o), calculated by fitting the Prandtl–von Karman logarithmic law to the measured wind speed profile. The shear velocity of wind was estimated using

$$u(z) = \frac{u^*}{0.4} \ln\left(\frac{z-d}{z_o}\right) \tag{3}$$

where $u(z)$ is wind velocity at height z, $u*$ is the shear velocity (or friction velocity), d is the zero-plane displacement, and 0.4 is the von Karman constant. Z_o is empirically determined by using the wind speeds at four heights (15-min events with average wind speed at 4 m height >8 m s^{-1}).

2.4. Sediment and Soil Sampling

Randomly distributed samples (approximately 10 g, total $n = 402$) from the top 5 cm of the soil were collected from each of the burned and control plots. This included 50 randomly distributed samples collected from one 5 × 5 m soil sampling plot from the burned and control areas. Each 5 × 5 m soil sampling plot was divided into 1 × 1 m grids to delineate soil sample location. To determine the relative contribution of wind erosion (mostly occurring during windy season from February to May) and water erosion (the region receives most of its precipitation from June to October) in redistributing sediment, soil samples were collected before and after each windy season. Samples were taken from the surface of bare microsites and under the vegetation canopies at shrub and grass microsites. For each of the randomly distributed sampling locations, the microsite type was recorded. These data were recorded to enable geostatistical analysis to determine the spatial patterns of sediment distribution. A

varying spatial pattern was used for each sampling interval to randomize the sampling strategy. In the year I, 26 samples were collected from each plot in each of the monitoring areas in the burned and control treatments. In addition, 50 additional samples were collected from one randomly selected plot in each treatment to investigate the fine scale spatial redistribution of tracers. In the year III, 15 samples were collected from each plot, and 50 additional samples were collected from the same plot in the burned and control treatment as in Year I. More information on the number of soil samples used for the REE analysis from each treatment and microsite type is provided in Supporting Information S1 (Tables S3–S5).

2.5. Rare Earth Element Tracer Analysis

After establishing the field site before the prescribed fire, three different REE were used at each microsite: holmium (Ho), ytterbium (Yb), and europium (Eu) on shrub, bare, and grass microsites, respectively. Target solutions of the REE oxides were prepared by dissolving in diluted nitric acid. By dissolving in nitric acid, the polyvalent REE cations could coat the particles and enter the exchange complex, which limits the leaching or winnowing from the soil matrix. The solution of REE oxides was sprayed onto the respective microsite and soil samples were collected periodically to determine the movement of sediment onsite. The soil and sediment samples were collected before and after each windy season occurring between March and June in Year I and III. The detailed methodology for REE tracer application is described elsewhere (Dukes et al., 2018). To determine the REE concentration of the soil and aeolian sediment samples, they were analyzed using EPA Method 3051A (2007). In this process, 2 g of sample was leached with concentrated HNO_3-HCl solution (9 mL of trace-metal-grade concentrated nitric acid and 3 mL of concentrated hydrochloric acid), predigested overnight to limit the pressure build-up, and then digested. In the microwave digestion (Microwave Digestion System, CEM MARS 6, Matthews, NC, USA) process, the samples were digested at 175°C for 30 min and the leachate was cooled to room temperature. The leachate was then filtered through No. 5 Whitman filter paper and vacuum filtered through 0.45 µm membrane. These filtered samples were then diluted to 50 mL to be analyzed on the Inductively Coupled Plasma Optical Emissions Spectrometry (ICP-OES) (iCAP™ 7200 spectrometer, Thermo Scientific, USA). To determine the contribution of aeolian sediment from each microsite, background REE concentrations were subtracted from sample REE concentrations, then normalized to the average spiked concentration minus the background (Table S2 in Supporting Information S1) Individual normalized sample concentrations were then divided by the sum of all normalized concentrations, yielding the percentage of each REE component.

A two-way ANOVA with no interaction term was used for the burned treatment and the control treatment to test for differences in REE concentrations of the aeolian sediment between years and tracers applied to the three microsite types. REE concentrations were log-transformed to approximate a more normal distribution. The robust linear model (rlm) analysis using the MASS package in *R* was performed on log-transformed REE concentrations of the soil samples to test for differences as a function of treatment, microsite, year, or interactions. Post-hoc tests to the rlm results were performed using the emmeans *R* package. Prior to log transformations of REE concentrations in aeolian sediment and soil samples, 0.001 ppm was added whenever the concentration was zero. This is justified as the detection limit of the ICP OES used for this analysis was 0.005 ppm.

2.6. Geostatistical Analysis

After determining the REE concentrations of the samples, the spatial distribution of REE tracers was quantified using geostatistical analysis. The spatial autocorrelation of the measured REE concentrations at different sample locations was represented by omnidirectional semivariograms, which depict the spatial dependence of samples as a function of separation distance (Sankey, Ravi, et al., 2012; Schlesinger et al., 1995; Wang et al., 2019). For these semivariograms, the spherical model was used to fit data (Li et al., 2008; Schlesinger et al., 1995) based on the following equations:

$$\gamma(h) = C_0 + \frac{1}{2}C\left[\frac{3h}{A_0} - \frac{h^3}{A_0^3}\right] \text{ when } h < A_0 \tag{4}$$

$$\gamma(h) = C_0 + C \text{ when } h > A_0 \tag{5}$$

where h is the lag interval, A_0 is range, C_0 is nugget variant, and C is structural variant. In semivariograms, the nugget represents the y-intercept of the plot, representing short-range error. The range is the variance of values

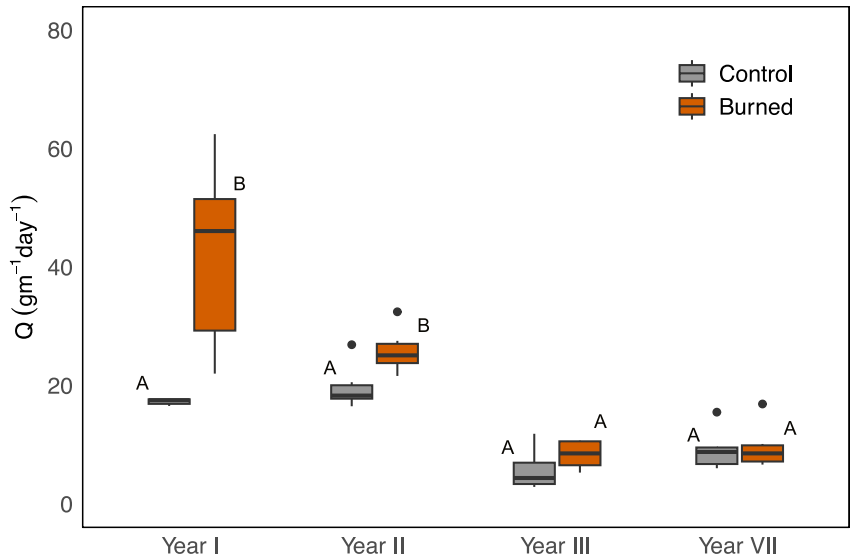

Figure 2. Total horizontal mass flux (Q) after each windy season post-fire from monitoring areas in the control ($n = 6$) and burned ($n = 6$) treatments. Different letters indicate significant differences in Q values in the year. Black dots represent outliers. The Q value of Year VII represents the average Q values for years IV–VII.

over the plot before reaching the sill ($C_0 + C$). This magnitude of spatial dependence ($C/C_0 + C$) is interpreted as correlated with the strength of autocorrelation among the data, where an increase in the ratio indicates stronger spatial autocorrelation (Li et al., 2008). Kriged maps were produced using the same parameters that were applied to the semivariograms.

3. Results

The burned plots had significantly greater Q values compared to the control plots in the first 2 years following the prescribed fire (Figure 2). However, the differences were not significantly different after 3 years. After the third windy season (June 2018), the Q values decreased in both the burned and control plots (Figure 2). Kruskal-Wallis one-way ANOVA on Ranks results indicate that the median Q values in June 2018 are not significantly different ($p > 0.1$) between the two plots, whereas in the other two collection periods (June 2016 and 2017) median Q values are significantly different between the control and burned plots ($p < 0.005$ and $p < 0.05$, respectively).

To observe the changes in surface roughness, the wind velocity values at the control and burned plots were used to estimate z_0, which relates to the height of surface roughness elements such as vegetation or microtopography. z_0 was significantly lower on the burned treatment compared to control during the first year (and windy season) after the fire. However, z_o increased after Year I in the burned treatment and did not differ significantly between treatments in all later years (Figure 3).

Aeolian sediments in the control plot in Year I contained greater proportions of bare microsite REE tracer (Yb) than the other two tracers, indicating that bare microsites are the dominant contributors of aeolian sediment in the control plot (Figure 4c). Among the three microsites, the shrub microsites (Ho) contributed the least (<2%) to aeolian sediments in the unburned areas. This pattern was consistent after 3 years (Figure 4c). During this 3-years period, the contribution of grass microsites to the aeolian sediments from the control areas ranged from 7% to 18%, indicating greater erosion compared to shrub microsites (Figure 4c). However, after the prescribed fire, the shrub microsites (38% ± 8%) along with the bare microsites (44% ± 9%) were a major contributor of aeolian sediments, a trend that remained consistent even after 3 years following fire (Figure 4c). Results of the two-way ANOVA conducted for the control treatment data in Figure 4a indicated that controlling for the three tracer and microsite types, concentrations did not differ significantly ($p > 0.05$) between Year I and III. Conversely, results of the two-way ANOVA conducted for the burned treatment data in Figure 4b indicated that controlling for the three tracer and microsite types, concentrations did differ significantly ($p < 0.05$) between Year I and III.

The REE tracer analysis of soil samples showed sediment mixing between the bare and grass microsites in the control plots, with both grass and shrub microsites being enriched with the bare tracer (Yb); the shrub tracer

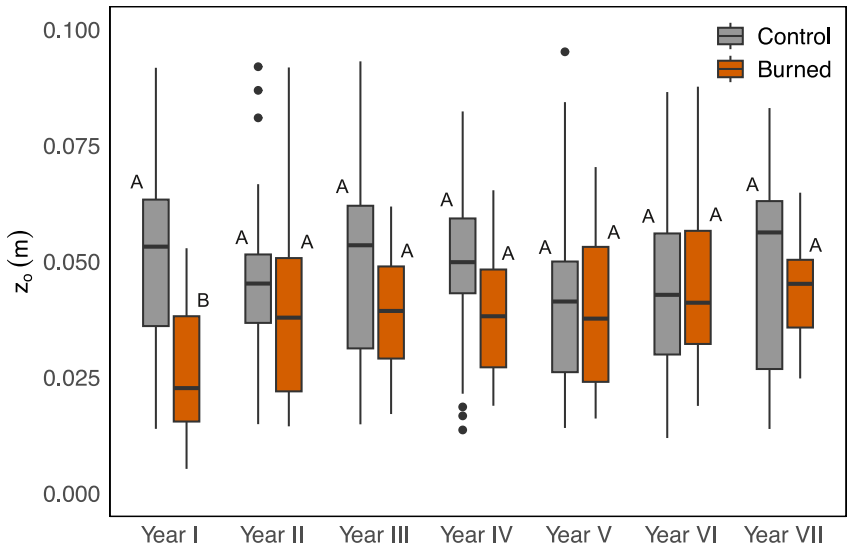

Figure 3. The variations in the derived aerodynamic roughness length (z_0) for the control and burned treatments. Different letters indicate significant differences in Z_o values in the year.

(Ho) mostly remained in shrub microsites (Figure 5). This pattern was consistent even after 3 years, with the bare site tracer (Yb) still contributing the most to all microsites; the grass and shrub tracers had lower concentrations than the bare tracer in all three microsites (Figure 5). Following 3 years (3 windy seasons), relative proportions of the three tracers at each microsite remained similar to the initial conditions of the control site. Bare microsites still had the highest concentration of bare tracers, followed by the grass and shrub tracers. Robust Linear Model and post-hoc test results showed significant differences between treatments, year, microsites, and interaction effects (treatment: year, year:microsite, and treatment: microsite) for all REE tracers. In Year I, Ho (shrub tracer) concentration was significantly greater in the bare microsites in the burned treatment compared to control ($p < 0.005$) but was not significantly different between treatments for other microsites. In Year III, Ho (shrub tracer) concentrations were significantly greater in both grass ($p < 0.001$) and bare ($p < 0.05$) microsites in the burned treatment, indicating a redistribution of sediments by wind from shrub microsites and capture by grass microsites. The Eu (grass tracer) and Yb (bare tracer) concentrations were not significantly different for any microsites between burned and control treatments in Year I. In Year III compared to Year I, the Yb concentration was significantly less for bare ($p < 0.05$) and shrub ($p < 0.05$) microsites, indicating possible export of sediment from the monitoring plots of both treatments as the bare soil was eroded by wind over time.

The soil samples from the burned plot immediately after the prescribed fire (March 2016) show patterns comparable to those of the control plot. The burned bare microsites again had the most variable REE concentrations in the soil, consisting mostly of bare tracer, followed by grass and shrub tracers. Burned grass microsites received some mixing from shrub tracers immediately after the fire but remained dominated by grass and bare tracers. Burned shrub microsites received little sediment input from grass microsites and consisted only of shrub and bare tracer concentrations (Figure S3 in Supporting Information S1).

After three windy seasons, the burned site exhibited considerable mixing between microsites. Bare microsites had major contributions from the bare tracer, followed by relatively similar amounts of grass and shrub tracer. Grass microsites had bare tracer as the major tracer, followed by similar amounts of grass and shrub tracers. Shrub microsites had slightly higher concentrations of the shrub tracer compared to other microsites, whereas bare and grass tracer remained at relatively similar concentrations. Over the course of the 3-years study, there is a significant decrease in soil and sediment REE concentrations in both control and burned plots, in some cases by more than half of the initial concentrations (Figure S3 in Supporting Information S1).

To assess the spatial variations in REE tracers in burned and control plots, kriged maps of REE concentrations were created for a selected replicate from burned and control treatments. Isotropic semivariograms were used for these data because there were no directional patterns found with anisotropic variograms at 0°, 45°, 90°, and 135°. The concentration of the shrub tracer (Ho) did not change in the control plot over 3 years, with the

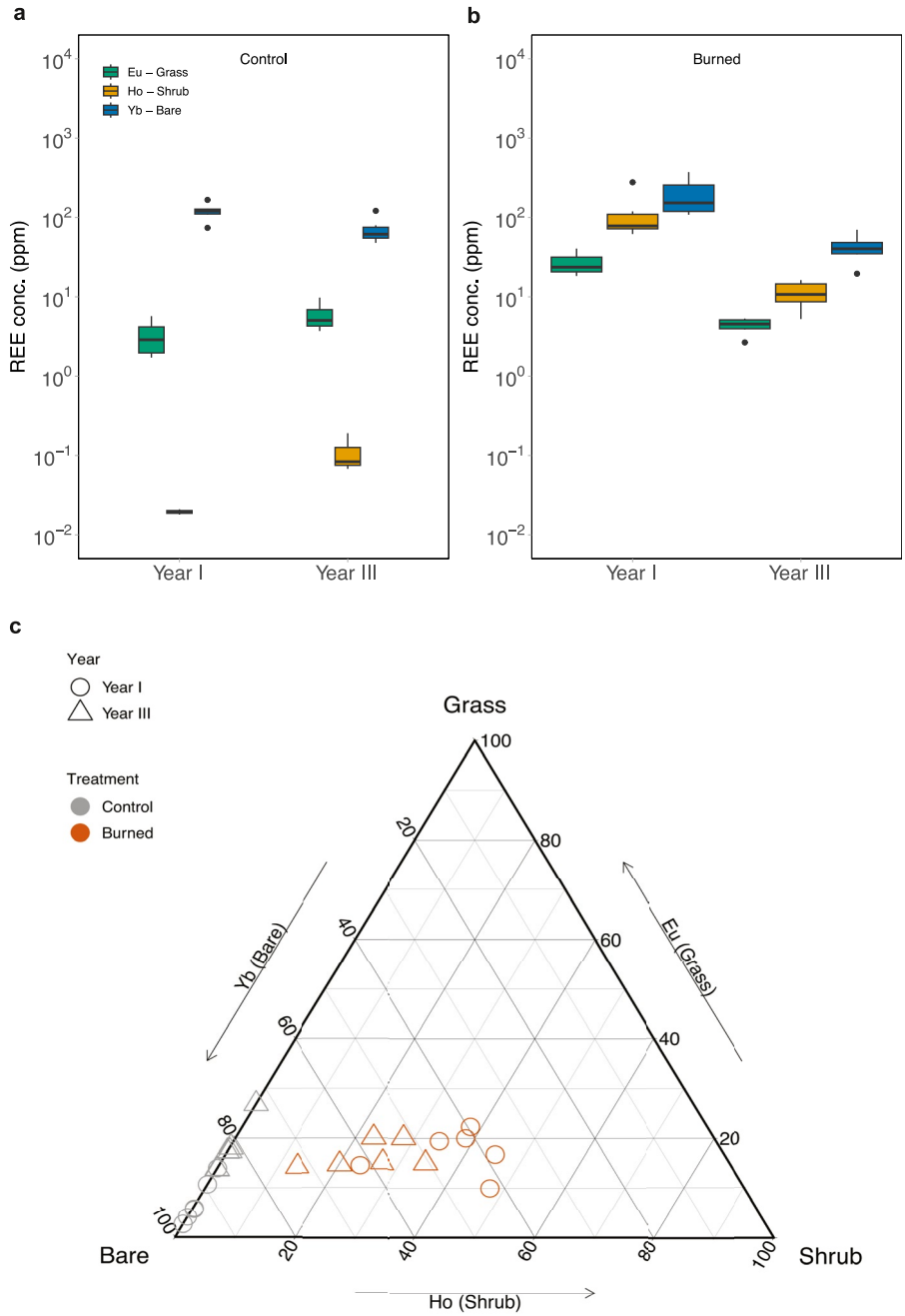

Figure 4. REE concentrations (ppm, log scale) of aeolian sediment samples in control ($n = 6$) and burned ($n = 6$) plots from two different collection periods: (a) Year I and (b) Year III. (c) Ternary diagrams of REE proportions from both control and burned plots from two sampling intervals. REE tracers: Eu, Ho, and Yb were initially applied to grasses, shrubs, and bare microsites, respectively.

tracer not being redistributed over the course of the experiment (Figure 6). In the burned plot, the shrub tracer (Ho) remained in a few locations as burned biomass immediately after the fire, but after three windy seasons, a more homogenous distribution of the tracer at the soil-sampling site was observed, indicating soil redistribution. The grass tracer (Eu) in the control plot was not redistributed and did not shift in position after 3 years, retained in mostly heterogeneous patches. In the burned plot immediately after the fire, the grass tracer (EU) remained in the plot as burned biomass yet to be removed from the plot, but after three windy seasons and sediment redistribution occurred, it appeared that grasses returned to the plot in the form of patchy cover. The

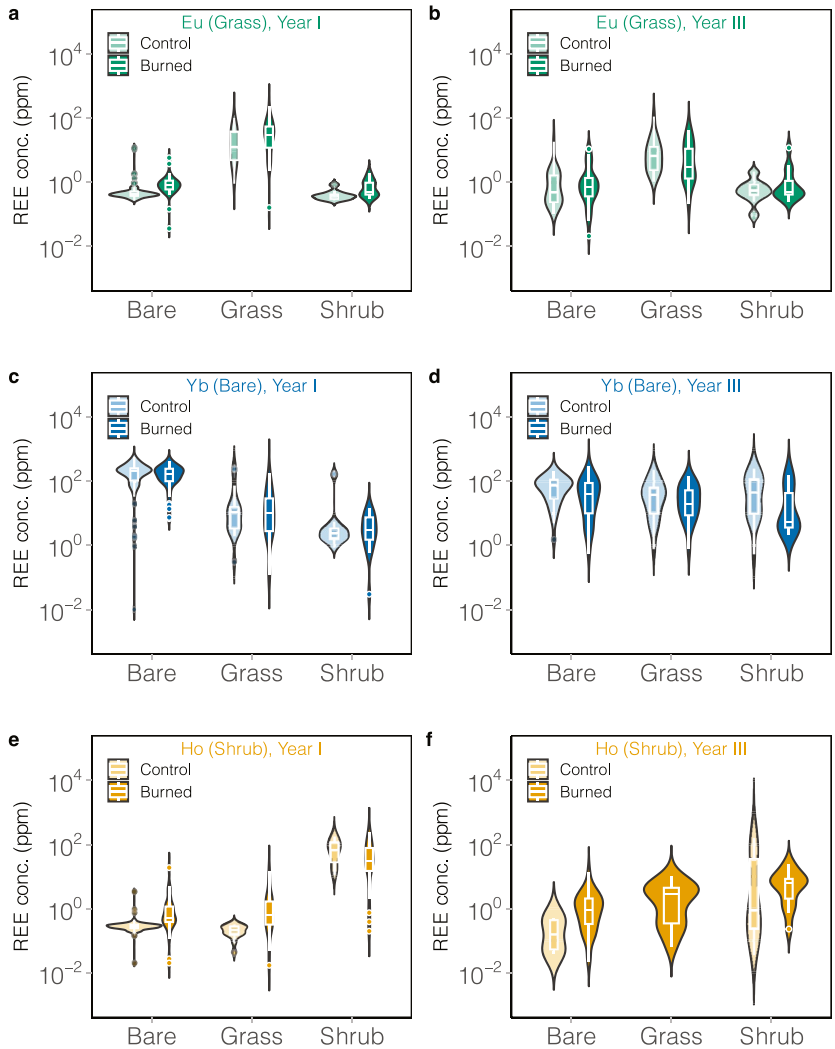

Figure 5. Concentrations (ppm, log scale) of rare earth element tracers in soil samples from different microsites in the control ($n = 208$) and burned ($n = 194$) areas from two different collection periods: Year I ($n = 242$) and Year III ($n = 160$). REE tracers: Eu, Ho, and Yb were initially applied to grass, shrub and bare microsites, respectively.

bare tracer (Figure S4–S6 in Supporting Information S1) was most spatially heterogeneous of all three. It was most susceptible to wind erosion, making it difficult to determine a trend in control or burned plots from either collection period.

A spherical isotropic model was used on the semivariograms, providing a good fit to the data. The range (A_0—distance of spatial autocorrelation) and the magnitude of spatial dependence [$C/(C_0 + C)$] of the semivariograms for the REE tracers in each plot from the beginning of the experimental period in March 2016 until June 2018 are presented in Supporting Information S1 (Table S6). Following three windy seasons, the autocorrelated distance for the shrub tracer (Ho) and the bare tracer (Yb) increased. The bare tracer increased slightly from 0.147 to 0.336 m, the shrub tracer increased by 1-m in the burned plot, and the grass tracer (Eu) decreased in autocorrelated distance by more than 1-m. In the control plot, both the shrub and grass tracers showed a decrease in autocorrelated distance by less than 0.5 m, while the bare tracer increased by 0.3 m. Over the three windy seasons, spatial dependence did not vary substantially in the three REE tracers. The only large variation was in the shrub tracer spatial dependence in the burned plot, which dropped from 99.8% to 58.0% after three windy seasons. A summary of the semivariogram model parameters for REE concentrations in control and burned plots over three windy seasons is provided in Supporting Information S1 (Table S6).

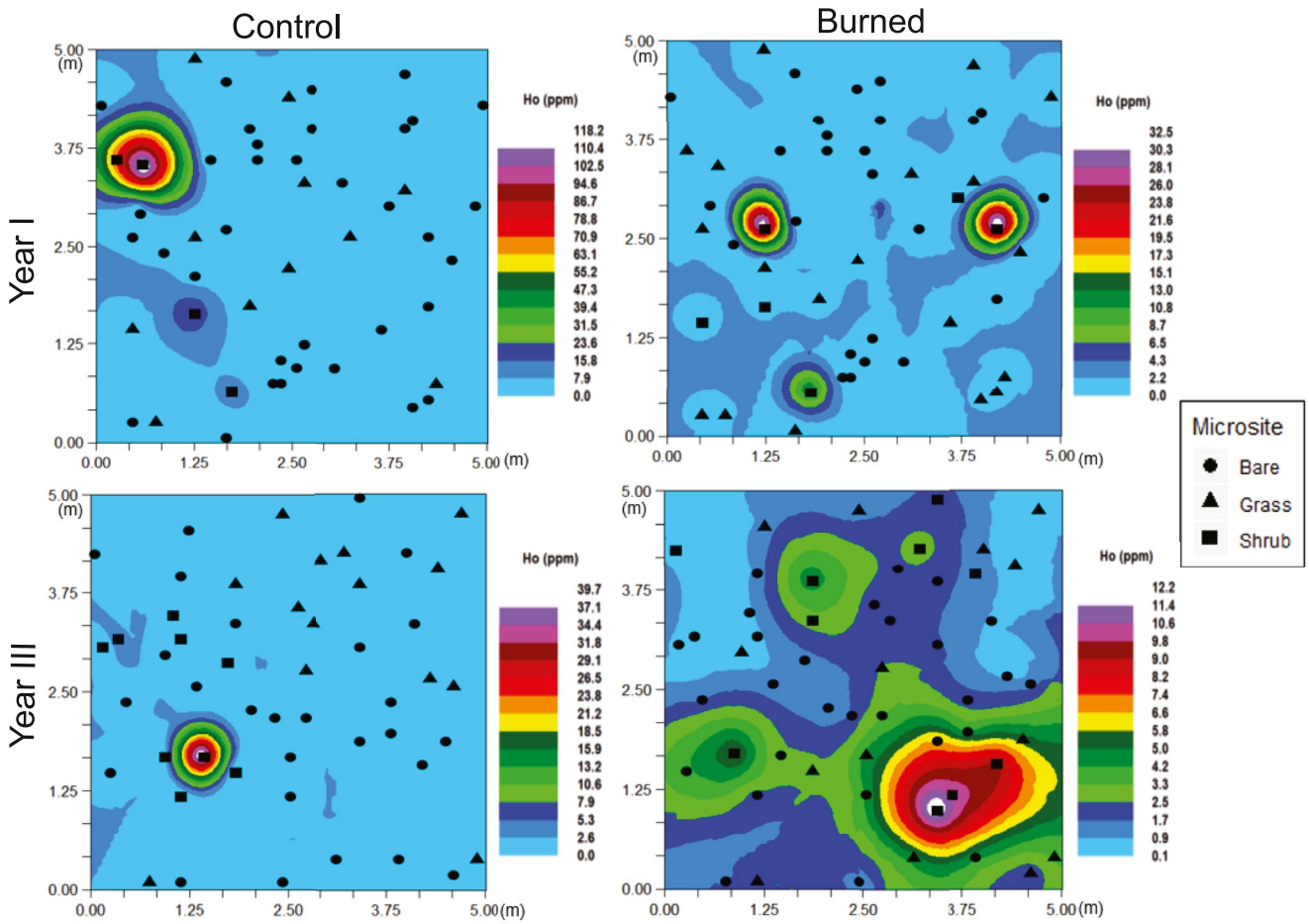

Figure 6. Kriged map of Ho concentrations (ppm) from soil samples taken from a control ($n = 50$) and burned ($n = 50$) plot from two different collection periods. Ho was initially applied to shrub microsites. Symbols on maps represent different microsites from which the soil sample was taken. Note the different concentration scales for each map.

4. Discussion

Our results indicate that the prescribed fire at the shrub-encroached grassland in the Chihuahuan Desert greatly accelerated the patch-scale aeolian transport and redistribution of sediments. After the first windy season following the fire, the total horizontal mass flux from aeolian sediment transport was three times greater in the burned plot compared with the control (Figure 2), indicating the enhancement of the aeolian erosion right after fire. Over the three windy seasons, however, there was a progressive decline in aeolian transport in the burned plot, and by year 3, the Q values from both plots showed no clear differences (Figure 2), which is consistent with previous studies (Ravi et al., 2012; Sankey et al., 2009). Fires accelerate erosion by altering two major controls on the wind erosion process—vegetation and soil moisture (Ravi, D'Odorico, Zobeck, et al., 2007; Ravi et al., 2006; Sankey, Germino, Sankey, & Hoover, 2012). Fires that remove vegetation decrease surface roughness (Figure 3), thereby increasing wind shear on the soil surface (Ravi et al., 2012; Sankey, Germino, & Glenn, 2012). Further, fires are known to induce soil water repellency (hydrophobicity) in vegetated microsites by releasing volatile organic compounds from vegetation and surface litter (DeBano, 2000; Doerr et al., 2000; Ravi et al., 2006). Fire-induced water repellency is known to increase wind erosion by decreasing the interparticle bonding forces due to moisture in soil (Ravi et al., 2006).

The decline in horizontal mass flux in the burned plots resulted from the observed recovery of grasses, and therefore surface roughness, along with the possible decline in soil water repellency after three windy seasons. Sankey et al. (2021) showed with UAV multispectral, and photogrammetry remote sensing conducted 6 months after the prescribed fire that bare soil, herbaceous (e.g., grass), and shrub cover were 78%, 15%, and 7%, respectively in

the burned area. This contrasted significantly with cover in the unburned control area that was 47%, 30%, and 23%, respectively, for bare soil, herbs, and shrubs (Sankey et al., 2021). Sankey et al. (2021) also showed with lidar remote sensing that some but not all individual shrubs had resprouted 1 year after the prescribed fire, and then grew in height and canopy cover between years one and two. Grasses and other herbs also expanded from almost no cover immediately after the fire (1 week) to extensive cover 2 years post-fire (Sankey et al., 2021). The lidar analysis additionally showed that the shrub and grass microsites eroded during the first-year post-fire fire due to the lack of vegetation cover but aggraded from sediment deposition beneath the canopies of regrown plants during the second-year post-fire (Sankey et al., 2021). Four years after a prescribed fire implemented in 2007 at the Sevilleta, Sankey, Ravi, et al. (2012) determined from lidar remote sensing that burned plots had statistically similar herbaceous biomass but >20 times less shrub biomass in comparison to unburned control plots.

REE tracer concentrations in the wind-blown sediment samples show that most sediments in the total horizontal mass flux from control plots were derived from the bare or grass microsites, with little contribution from shrub microsites (Figure 4), demonstrating the expected sediment feedback manifested using the shrub encroachment process in grasslands (Wang et al., 2019). This observation agrees with traditional theory of fertility islands (Charley & West, 1975; Schlesinger et al., 1990) stating that the increased entrainment of sediments from the bare and grass microsites combined with the sheltering and trapping of sediments by shrub canopy reinforce landscape heterogeneity and contribute to the development of islands of enhanced hydrological and biological productivity. The shrub islands may also accumulate more water from precipitation by higher infiltration rates compared to bare and grass microsites (Duniway et al., 2018; Gonzales et al., 2018; Ravi, D'Odorico, & Okin, 2007). Conversely, the degrading grass vegetation in the interspaces may not be able to increase threshold shear velocity enough to prevent soil from being eroded, as indicated by sediment mixing occurring between grass and bare microsites. Thus, the increased entrainment of sediments from the bare and grass microsites combined with the sheltering and trapping of sediments by shrub canopy enhances and maintains the islands of fertility in shrub encroached landscapes.

The reintroduction of fire in the shrub-grass system resulted in considerable changes in the vegetation-sediment feedback, as indicated by the variations in REE tracer concentrations between the control and the burned plots. The burned area had a large increase in sediment contribution from the shrub microsites that coincided with a decrease in sediment contribution from grass and bare microsites (Figure 4c). The large increase in aeolian sediment from shrub microsites can be attributed to the loss of vegetation and the hydrophobicity of the soil post-fire. Previous studies have demonstrated the role of fire-induced water repellency in enhancing aeolian transport in these desert grasslands (Ravi et al., 2009) following fires. Fire-induced soil water repellency is typically greater under shrub vegetation and is generally short lived in these systems, often disappearing after the rainy season (Ravi et al., 2009). Removing vegetation and thus reducing the microtopographic relief (elevation) and inducing water repellency on the burned plot soil allows for patch-scale acceleration of aeolian sediment transport and subsequent mixing between all the three microsites. This shift transforms shrub microsites from sediment sinks to sources in the burned areas, thereby allowing for potential spatial homogenization of soil resources (nutrients and water) in the landscape, thus reversing the nutrient feedback that reinforces the shrub state (Bird et al., 2002; Dukes et al., 2018; Ravi et al., 2009; Sankey et al., 2021; Wang et al., 2019).

Tracer concentration in the soil samples (Figure 5) and kriged maps of REE concentrations (Figure 6) in the burned plot further support evidence of increased soil spatial homogeneity following prescribed fire. Initial site conditions on the kriged maps show a heterogeneous landscape; specifically with the shrub microsite tracer, there were three isolated concentrations of holmium (shrub microsites), indicating a strong fertility island effect. After the fire, there was an overall decrease in holmium concentration in the sampling area, but the sediment redistribution after three windy seasons led to a more homogeneous distribution of this tracer throughout the site. Geostatistical analysis also supports the redistribution of soil nutrients via the holmium tracer on the burned site, with spatial autocorrelation increasing by 1 m over three windy seasons (Table S6 in Supporting Information S1). Specifically, europium decreases in spatial autocorrelation in both control and burned plots, meaning most of the tracer may have eroded out of the monitoring areas (Table S6 in Supporting Information S1).

Our results suggest that an efficient prescribed burn process in the Chihuahuan Desert has been seen to work over a 7-years interval, comparable to the historical fire return intervals in the Chihuahuan desert grasslands (Drewa et al., 2001; McPherson, 1995). It is important to consider confounding factors that will impact the effectiveness of the controlled burn. The age of the shrub may affect fire-induced mortality. Fires followed by

droughts or extreme wind and rainfall events may result in net sediment and nutrient loss rather than sediment redistribution of those resources (Hasselquist et al., 2011; Sankey, Germino, Benner et al., 2012), decreasing the chance of grass recovery in the system. Frequent fires can result in higher background sediment yields if grass recovery is impeded by moisture stress or reduced soil quality caused by accelerated erosion (Ravi et al., 2012; Shakesby & Doerr, 2006). Post-fire soil moisture conditions (precipitation) are crucial for the recovery of grasses to the system to maintain soil moisture for grass establishment (Drewa & Havstad, 2001; Parker et al., 2022). Further studies are needed to address some of the concerns regarding REE-based sediment tracing method for long-term studies, including the effects of different REE application methods, selectivity of the REE binding to different soil aggregates, and the potential leaching and loss of REE tracers from the application area. Soil textural differences, even between microsites, can be significant in some sites and need to be addressed. For soil with higher clay content, the samples should be separated into sub-samples of aggregate sizes that present homogeneous binding of REE. However, these techniques can greatly increase the time, cost and complexity of the analysis (Guzman et al., 2013; Kimoto et al., 2006; Zhang et al., 2001).

5. Conclusions

Our study examined the microsite scale interactions among fire, wind, vegetation, and soil erosion processes in a shrub-encroached grassland using long-term field observations of aeolian sediment transport and a multi-tracer approach to monitor the sediment sources and sinks. In the shrub-encroached grassland, a prescribed fire significantly increased soil erosion rates from vegetated sites, leading to a redistribution of soil nutrients that favors grass and bare microsites over shrub microsites. Increasing homogeneity in the distribution of vegetation as well as an increase in surface roughness over three windy seasons indicated the reestablishment of grass cover. This shift in vegetation was likely an indication of the reversal of the nutrient feedback that supported shrub encroachment, with fire impact shifting shrubs from soil nutrient sinks to sources. Increasing population and changing climate will shift land use in several regions across the world, potentially increasing aridity in dryland systems and changing frequency and intensity of wildfires, which could then lead to the acceleration of aeolian soil erosion in dryland systems. However, this research highlights the role of prescribed fires in shrub encroached grasslands as an effective land management tool that can leverage post-fire aeolian sediment transport to potentially improve the condition of desert grasslands in the future.

Conflict of Interest

The authors declare no conflicts of interest relevant to this study.

Data Availability Statement

All data used in our work can be found online Burger et al. (2023) (https://doi.org/10.6084/m9.figshare.24153420.v1).

Acknowledgments
This research was funded by the U.S. National Science Foundation (NSF) Award EAR-1451518 for S. Ravi, Award EAR- 1451489 for J. Li, and the Sevilleta LTER Faculty Summer Research Fellowship for S. Ravi. The authors gratefully acknowledge the contributions of Jon Erz & Andy Lopez (FWS, SNWR), Scott Collins and Jennifer Rudgers (Sevilleta LTER, New Mexico, USA) for providing access to field and laboratory facilities and technical guidance. USDA is an equal opportunity employer and provider. J. B. Sankey was additionally supported by the USGS Ecosystems Mission Area. This manuscript is submitted for publication with the understanding that the U.S. Government is authorized to reproduce and distribute reprints for Governmental purposes. Any use of trade, product, or firm names is for descriptive purposes only and does not imply endorsement by the U.S. Government.

References

Archer, S. (1989). Have southern Texas savannas been converted to woodlands in recent history? *The American Naturalist*, *134*(4), 545–561. https://doi.org/10.1086/284996

Archer, S., Schimel, D. S., & Holland, E. A. (1995). Mechanisms of shrubland expansion: Land use, climate or CO_2? *Climatic Change*, *29*(1), 91–99. https://doi.org/10.1007/BF01091640

Bird, S. B., Herrick, J. E., Wander, M. M., & Wright, S. F. (2002). Spatial heterogeneity of aggregate stability and soil carbon in semi-arid rangeland. *Environmental Pollution*, *116*(3), 445–455. https://doi.org/10.1016/S0269-7491(01)00222-6

Breshears, D. D., Whicker, J. J., Johansen, M. P., & Pinder, J. E. (2003). Wind and water erosion and transport in semi-arid shrubland, grassland and forest ecosystems: Quantifying dominance of horizontal wind-driven transport. *Earth Surface Processes and Landforms*, *28*(11), 1189–1209. https://doi.org/10.1002/esp.1034

Burger, W. J., Van Pelt, S., Grandstaff, D., Wang, G., Sankey, T., Li, J., et al. (2023). Sev REE project 2023 [Dataset]. figshare. https://doi.org/10.6084/m9.figshare.24153420.v1

Charley, J. L., & West, N. E. (1975). Plant-induced soil chemical patterns in some shrub-dominated semi-desert ecosystems of Utah. *Journal of Ecology*, *63*(3), 945–963. https://doi.org/10.2307/2258613

Deasy, C., & Quinton, J. N. (2010). Use of rare Earth oxides as tracers to identify sediment source areas for agricultural hillslopes. *Solid Earth*, *1*(1), 111–118. https://doi.org/10.5194/se-1-111-2010

DeBano, L. F. (2000). The role of fire and soil heating on water repellency in wildland environments: A review. *Journal of Hydrology*, *231*(2000), 195–206. https://doi.org/10.1016/S0022-1694(00)00194-3

D'Odorico, P., Bhattachan, A., Davis, K. F., Ravi, S., & Runyan, C. W. (2013). Global desertification: Drivers and feedbacks. *Advances in Water Resources*, *51*, 326–344. https://doi.org/10.1016/j.advwatres.2012.01.013

Doerr, S. H., Shakesby, R. A., & Walsh, R. P. D. (2000). Soil water repellency: Its causes, characteristics and hydro-geomorphological significance. *Earth-Science Reviews*, *51*(1–4), 33–65. https://doi.org/10.1016/S0012-8252(00)00011-8

Drewa, P. B., & Havstad, K. M. (2001). Effects of fire, grazing, and the presence of shrubs on Chihuahuan desert grasslands. *Journal of Arid Environments*, *48*(4), 429–443. https://doi.org/10.1006/jare.2000.0769

Drewa, P. B., Peters, D. P. C., & Havstad, K. M. (2001). Fire, grazing, and honey mesquite invasion in black grama-dominated grasslands of the Chihuahuan Desert: A synthesis. In K. E. M. Galley, & T. P. Wilson (Eds.), *Proceedings of the invasive species workshop: The role of fire in the control and spread of invasive species. Fire conference 2000: The first national congress on fire ecology, prevention, and management*. Miscellaneous Publication No. 11. Tall Timbers Research Station.

Dukes, D., Gonzales, H. B., Ravi, S., Grandstaff, D. E., Van Pelt, R. S., Li, J., et al. (2018). Quantifying postfire aeolian sediment transport using rare earth element tracers. *Journal of Geophysical Research: Biogeosciences*, *123*(1), 288–299. https://doi.org/10.1002/2017JG004284

Duniway, M. C., Petrie, M. D., Peters, D. P. C., Anderson, J. P., Crossland, K., & Herrick, J. E. (2018). Soil water dynamics at 15 locations distributed across a desert landscape: Insights from a 27-yr dataset. *Ecosphere*, *9*(7), e02335. https://doi.org/10.1002/ecs2.2335

Field, J. P., Belnap, J., Breshears, D. D., Neff, J. C., Okin, G. S., Whicker, J. J., et al. (2010). The ecology of dust. *Frontiers in Ecology and the Environment*, *8*(8), 423–430. https://doi.org/10.1890/090050

Field, J. P., Breshears, D. D., & Whicker, J. J. (2009). Toward a more holistic perspective of soil erosion: Why aeolian research needs to explicitly consider fluvial processes and interactions. *Aeolian Research*, *1*(1–2), 9–17. https://doi.org/10.1016/j.aeolia.2009.04.002

Gillette, D. A., & Pitchford, A. M. (2004). Sand flux in the northern Chihuahuan desert, New Mexico, USA, and the influence of mesquite-dominated landscapes. *Journal of Geophysical Research*, *109*(F4), F04003. https://doi.org/10.1029/2003JF000031

Gonzales, H. B., Ravi, S., Li, J., & Sankey, J. B. (2018). Ecohydrological implications of aeolian sediment trapping by sparse vegetation in drylands: Aeolian sediment trapping by dryland vegetation. *Ecohydrology*, *11*(7), e1986. https://doi.org/10.1002/eco.1986

Grover, H. D., & Musick, H. B. (1990). Shrubland encroachment in southern New Mexico, U.S.A.: An analysis of desertification processes in the American southwest. *Climatic Change*, *17*(2–3), 305–330. https://doi.org/10.1007/BF00138373

Guzman, G., Quinton, J. N., Nearing, M., Mabit, L., & Gómez, J. A. (2013). Sediment tracers in water erosion studies: Current approaches and challenges. *Journal of Soils and Sediments*, *13*(4), 816–833. https://doi.org/10.1007/s11368-013-0659-5

Hasselquist, N. J., Germino, M. J., Sankey, J. B., Ingram, L. J., & Glenn, N. F. (2011). Aeolian nutrient fluxes following wildfire in sagebrush steppe: Implications for soil carbon storage. *Biogeosciences*, *8*(12), 3649–3659. https://doi.org/10.5194/bg-8-3649-2011

Higgins, R. W., Yao, Y., & Wang, X. L. (1997). Influence of the North American monsoon system on the US summer precipitation regime. *Journal of Climate*, *10*(10), 2600–2622. https://doi.org/10.1175/1520-0442(1997)010<2600:IOTNAM>2.0.CO;2

Huxman, T. E., Wilcox, B. P., Breshears, D. D., Scott, R. L., Snyder, K. A., Small, E. E., et al. (2005). Ecohydrological implications of woody plant encroachment. *Ecology*, *86*(2), 308–319. https://doi.org/10.1038/s41467-017-02620-y

Kimoto, A., Nearing, M. A., Zhang, X. C., & Powell, D. M. (2006). Applicability of rare earth element oxides as sediment tracers for coarse textured soils. *Catena*, *65*(3), 214–222. https://doi.org/10.1016/j.catena.2005.10.002

Kok, J. F., Ward, D. S., Mahowald, N. M., & Evan, A. T. (2018). Global and regional importance of the direct dust-climate feedback. *Nature Communications*, *9*(1), 241. https://doi.org/10.1038/s41467-017-02620-y

Li, J., Okin, G. S., Alvarez, L., & Epstein, H. (2007). Quantitative effects of vegetation cover on wind erosion and soil nutrient loss in a desert grassland of southern New Mexico, USA. *Biogeochemistry*, *85*(3), 317–332. https://doi.org/10.1007/s10533-007-9142-y

Li, J., Okin, G. S., Alvarez, L., & Epstein, H. (2008). Effects of wind erosion on the spatial heterogeneity of soil nutrients in two desert grassland communities. *Biogeochemistry*, *88*(1), 73–88. https://doi.org/10.1007/s10533-008-9195-6

Li, J., Ravi, S., Wang, G., Van Pelt, R. S., Gill, T. E., & Sankey, J. B. (2022). Woody plant encroachment of grassland and the reversibility of shrub dominance: Erosion, fire, and feedback processes. *Ecosphere*, *13*(3), e3949. https://doi.org/10.1002/ecs2.3949

McPherson, G. R. (1995). The role of fire in the desert grasslands. In M. P. McClaran, & T. R. Van Devender (Eds.), *The desert grassland*. University of Arizona Press.

Millennium Ecosystem Assessment. (2005). *Ecosystems and human well-being: Synthesis*. Island Press.

Munson, S. M., Belnap, J., & Okin, G. S. (2011). Responses of wind erosion to climate-induced vegetation changes on the Colorado Plateau. *Proceedings of the National Academy of Sciences of the United States of America*, *108*(10), 3854–3859. https://doi.org/10.1073/pnas.1014947108

Okin, G. S., & Gillette, D. A. (2001). Distribution of vegetation in wind-dominated landscapes: Implications for wind erosion modeling and landscape processes. *Journal of Geophysical Research*, *106*(D9), 9673–9683. https://doi.org/10.1029/2001JD900052

Okin, G. S., Gillette, D. A., & Herrick, J. E. (2006). Multi-scale controls on and consequences of aeolian processes in landscape change in arid and semi-arid environments. *Journal of Arid Environments*, *65*(2), 253–275. https://doi.org/10.1016/j.jaridenv.2005.06.029

Okin, G. S., Parsons, A. J., Wainwright, J., Herrick, J. E., Bestelmeyer, B. T., Peters, D. C., & Fredrickson, E. L. (2009). Do Changes in connectivity explain desertification? *BioScience*, *59*(3), 237–244. https://doi.org/10.1525/bio.2009.59.3.8

Parker, N. J., Sullins, D. S., Haukos, D. A., Fricke, K. A., & Hagen, C. A. (2022). Recovery of working grasslands following a megafire in the southern mixed-grass prairie. *Global Ecology and Conservation*, *36*, e02142. https://doi.org/10.1016/j.gecco.2022.e02142

Polyakov, V. O., & Nearing, M. A. (2004). Rare earth element oxides for tracing sediment movement. *Catena*, *55*(3), 255–276. https://doi.org/10.1016/S0341-8162(03)00159-0

Ravi, S., Baddock, M. C., Zobeck, T. M., & Hartman, J. (2012). Field evidence for differences in post-fire aeolian transport related to vegetation type in semi-arid grasslands. *Aeolian Research*, *7*, 3–10. https://doi.org/10.1016/j.aeolia.2011.12.002

Ravi, S., D'Odorico, P., Breshears, D. D., Field, J. P., Goudie, A. S., Huxman, T. E., et al. (2011). Aeolian processes and the biosphere. *Reviews of Geophysics*, *49*(3), 1–45. https://doi.org/10.1029/2010RG000328

Ravi, S., D'Odorico, P., Herbert, B., Zobeck, T., & Over, T. M. (2006). Enhancement of wind erosion by fire-induced water repellency. *Water Resources Research*, *42*(11), W11422. https://doi.org/10.1029/2006WR004895

Ravi, S., D'Odorico, P., & Okin, G. S. G. S. (2007). Hydrologic and aeolian controls on vegetation patterns in arid landscapes. *Geophysical Research Letters*, *34*(24), L24S23. https://doi.org/10.1029/2007GL031023

Ravi, S., D'Odorico, P., Wang, L., White, C. S., Okin, G. S., Macko, S. A., & Collins, S. L. (2009). Post-fire resource redistribution in desert grasslands: A possible negative feedback on land degradation. *Ecosystems*, *12*(3), 434–444. https://doi.org/10.1007/s10021-009-9233-9

Ravi, S., D'Odorico, P., Zobeck, T. M., Over, T. M., & Collins, S. L. (2007). Feedbacks between fires and wind erosion in heterogeneous arid lands. *Journal of Geophysical Research*, *112*(G4), 1–7. https://doi.org/10.1029/2007JG000474

Sankey, J. B., Germino, M. J., Benner, S. G., Glenn, N. F., & Hoover, A. N. (2012). Transport of biologically important nutrients by wind in an eroding cold desert. *Aeolian Research*, *7*, 17–27. https://doi.org/10.1016/j.aeolia.2012.01.003

Sankey, J. B., Germino, M. J., & Glenn, N. F. (2009). Aeolian sediment transport following wildfire in sagebrush steppe. *Journal of Arid Environments*, *73*(10), 912–919. https://doi.org/10.1016/j.jaridenv.2009.03.016

Sankey, J. B., Germino, M. J., & Glenn, N. F. (2012). Dust supply varies with sagebrush microsites and time since burning in experimental erosion events. *Journal of Geophysical Research*, *117*(G1), G01013. https://doi.org/10.1029/2011JG001724

Sankey, J. B., Germino, M. J., Sankey, T. T., & Hoover, A. N. (2012). Fire effects on the spatial patterning of soil properties in sagebrush steppe, USA: A meta-analysis. *International Journal of Wildland Fire*, *21*(5), 545–556. https://doi.org/10.1071/WF11092

Sankey, J. B., Ravi, S., Wallace, C. S., Webb, R. H., & Huxman, T. E. (2012). Quantifying soil surface change in degraded drylands: Shrub encroachment and effects of fire and vegetation removal in a desert grassland. *Journal of Geophysical Research*, *117*(G2), G02025. https://doi.org/10.1029/2012JG002002

Sankey, J. B., Sankey, T. T., Li, J., Ravi, S., Wang, G., Caster, J., & Kasprak, A. (2021). Quantifying plant-soil-nutrient dynamics in rangelands: Fusion of UAV hyperspectral-LiDAR, UAV multispectral-photogrammetry, and ground-based LiDAR-digital photography in a shrub-encroached desert grassland. *Remote Sensing of Environment*, *253*, 112223. https://doi.org/10.1016/j.rse.2020.112223

Schlesinger, W. H., Raikes, J. A., Hartley, A. E., & Cross, A. F. (1995). On the spatial pattern of soil nutrients in desert ecosystems: Ecological archives E077-002. *Ecology*, *77*(2), 364–374. https://doi.org/10.2307/2265615

Schlesinger, W. H., Reynolds, J. F., Cunningham, G. F., Huenneke, L. F., Jarrell, W. M., Virginia, R. A., & Whitford, W. G. (1990). Biological feedbacks in global desertification. *Science*, *247*(4946), 1043–1048. https://doi.org/10.1126/science.247.4946.1043

Shakesby, R. A., & Doerr, S. H. (2006). Wildfire as a hydrological and geomorphological agent. *Earth-Science Reviews*, *74*(3), 269–307. https://doi.org/10.1016/j.earscirev.2005.10.006

Shao, Y., & Raupach, M. R. (1992). The overshoot and equilibration of saltation. *Journal of Geophysical Research*, *97*(D18), 20559–20564. https://doi.org/10.1029/92JD02011

Shao, Y., Raupach, M. R., & Findlater, P. A. (1993). Effect of saltation bombardment on the entrainment of dust by wind. *Journal of Geophysical Research*, *98*(D7), 12719–12726. https://doi.org/10.1029/93JD00396

Sterk, G., & Raats, P. A. C. (1996). *Wind erosion in the Sahelian zone of Niger: Processes, models, and control techniques* (p. 152). Wageningen Agricultural University.

Turnbull, L., Wilcox, B., Belnap, J., Ravi, S., D'Odorico, P., Childers, D., et al. (2012). Understanding the role of ecohydrological feedbacks in ecosystem state change in drylands. *Ecohydrology*, *5*(2), 174–183. https://doi.org/10.1002/eco.265

Van Auken, O. W. (2000). Shrub invasions of North American semiarid grasslands. *Annual Review of Ecology and Systematics*, *31*(1), 197–215. https://doi.org/10.1146/annurev.ecolsys.31.1.197

Wang, G., Li, J., Ravi, S., Dukes, D., Gonzales, H. B., & Sankey, J. B. (2019). Post-fire redistribution of soil carbon and nitrogen at a grassland–shrubland ecotone. *Ecosystems*, *22*(1), 174–188. https://doi.org/10.1007/s10021-018-0260-2

Wang, G., Li, J., Ravi, S., Scott Van Pelt, R., Costa, P. J. M., & Dukes, D. (2017). Tracer techniques in aeolian research: Approaches, applications, and challenges. *Earth-Science Reviews*, *170*, 1–16. https://doi.org/10.1016/j.earscirev.2017.05.001

Wilcox, B. P. (2010). Transformative ecosystem change and ecohydrology: Ushering in a new era for watershed management. *Ecohydrology*, *3*(1), 126–130. https://doi.org/10.1002/eco.104

Wolfe, S. A., & Nickling, W. G. (1993). The protective role of sparse vegetation in wind erosion. *Progress in Physical Geography: Earth and Environment*, *17*(1), 50–68. https://doi.org/10.1177/030913339301700104

Zhang, X. C., Friedrich, J. M., Nearing, M. A., & Norton, L. D. (2001). Potential use of rare Earth oxides as tracers for soil erosion and aggregation studies. *Soil Science Society of America Journal*, *65*(5), 1508–1515. https://doi.org/10.2136/sssaj2001.6551508x

Erratum

The originally published version of this article contained a typographical error. All instances of the term "rare Earth element" have been corrected to "rare earth element." This may be considered the authoritative version of record.